UvA-DARE (Digital Academic Repository)

Reversible multi-electron storage in dual-site redox-active supramolecular cages

Plessius, R.; Orth, N.; Ivanović-Burmazović, I.; Siegler, M.A.; Reek, J.N.H.; van der Vlugt, J.I.

Citation for published version (APA):

Plessius, R., Orth, N., Ivanović-Burmazović, I., Siegler, M. A., Reek, J. N. H., & van der Vlugt, J. I. (2019). Reversible multi-electron storage in dual-site redox-active supramolecular cages. *Chemical Communications*, *55*(84), 12619-12622. https://doi.org/10.1039/c9cc07138e

Reversible multi-electron storage in dual-site redox-active supramolecular cages†

Raoul Plessius,[a] Nicole Orth,[b] Ivana Ivanović-Burmazović,[b] Maxime A. Siegler,[c] Joost N. H. Reek [iD] *[a] and Jarl Ivar van der Vlugt [iD] *[a]

$M_6L_4^{12+}$ supramolecular cages 3a and 3b (M = Pd, Pt), soluble in organic solvents, contain two different ligand-centered redox sites that enable the reversible storage of up to 16 electrons, as probed by CV, UV/vis spectro-electrochemistry (SEC-UV/Vis), bulk electrolysis and EPR. Encapsulation of a $B_{12}F_{12}^{2-}$ anion is confirmed by ^1H, ^{19}F NMR and ^{19}F DOSY NMR spectroscopy and mass spectrometry.

Supramolecular strategies are widely used in chemistry to make well-defined large architectures. Non-covalent self-assembly involving metal ions and rationally designed organic linkers provides a robust and modular method for the synthesis of a variety of porous structures.[1–11] These porous structures are regularly exploited as static containers to accommodate guest molecules. In addition, they have been demonstrated to be useful for catalysis, displaying effects such as catalyst stabilization,[12] enhancement of the rate and/or selectivity of a reaction,[13,14] selective activation of organometallic precursors[15] or modification of the reaction mechanism.[16] Selective encapsulation[17,18] and one-pot cascade reactions[19] with spatially isolated systems have also been reported.

The incorporation of stimuli-responsive components into self-assembled cages to access dynamic containers that can (reversibly) undergo electronic or structural changes has recently gained momentum, as this may allow further control over chemical events in complex mixtures.[20–22] The use of light-sensitive or redox-active components that react to an external stimulus are two prevalent concepts to integrate stimulus responsivity within the design of self-assembled supramolecular architectures. The use of redox-active components for switching requires systems that undergo

reversible redox event(s). Recent contributions include a small $M_2L_4^{4+}$ capsule with 'single-site' redox-active walls,[23] allowing for an overall charge switching from 4+ to 8+, two M_4L_2 capsules with control over encapsulation properties via redox-stimuli[24,25] and a large $M_4L_6^{8+}$ assembly containing redox-active perylene bisimide (PBI) struts and Fe-bipyridine linkers, with postulated cycling between 18+ and 16− charged species.[26]

Fujita-type $M_6L_4^{12+}$ supramolecular cages are easy to prepare, they can bind a wide variety of guests and facilitate selective transformations of encapsulated species.[27] These highly cationically charged containers typically feature redox-inert Pd (or Pt) diamine metal nodes linked by C_3-symmetric panels. We considered to incorporate redox-active ligands into the metal nodes to enrich the redox chemistry of envisioned cages.[28] The bis(arylimino)-acenaphthene (BIAN) motif is well suited, as it displays three well-defined redox-states adi, aia⁻• and ada²⁻ upon coordination to a transition metal (Fig. 1, top).[29]

We herein report Fujita-type M_6L_4 metallocages, featuring redox-active BIAN-ligands, that show multiple reversible reductive redox events. Platinum is found to provide superior redox-stability for the resulting cages compared to palladium. The redox-active C_3-symmetric trispyridyltriazine (tpt) panels of these M_6L_4 cages are a second electro-responsive site (Fig. 1, bottom). The presence of two distinctly different redox-sites provides supramolecular assemblies that can be reversibly switched over 16 charge units, as deduced
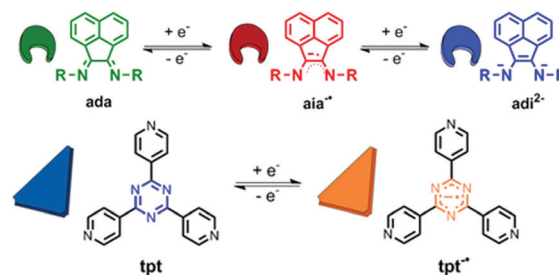
[a] van't Hoff Institute for Molecular Sciences, University of Amsterdam, Science Park 904, Amsterdam, The Netherlands. E-mail: j.n.h.reek@uva.nl, j.i.vandervlugt@uva.nl

[b] Department of Chemistry und Pharmacy, Friedrich Alexander Universität Erlangen-Nürnberg, Egerlandstrasse 1, 91058 Erlangen, Germany

[c] Department of Chemistry, John Hopkins University, Baltimore, MD 21218, USA

† Electronic supplementary information (ESI) available. CCDC 1923049 and 1923050. For ESI and crystallographic data in CIF or other electronic format see DOI: 10.1039/c9cc07138e
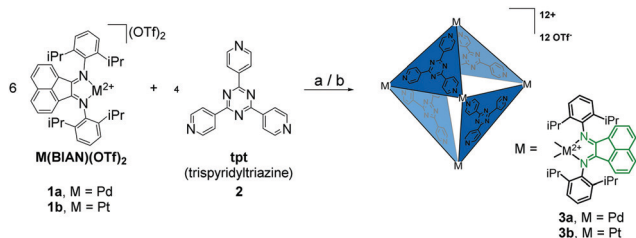

Fig. 1   Representation of redox-states of (top) the BIAN-motif, going from left to right and (bottom) trispyridyl triazine (tpt).

Scheme 1 Synthesis of redox-active metallocages featuring two distinctly different redox-active sites **3a** and **3b**. Conditions for (a) DCM, 1 hour at room temperature, (b) DCM/MeCN, 3 days at 40 °C.

from coulometry, MS and EPR spectroscopic data. The combined data suggest no electronic communication between the different redox-loci. We also report initial guest encapsulation studies with these new cages that are soluble in organic solvents.

Metallocages **3a** and **3b** with triflate counterions are obtained by mixing of the respective building blocks [M(BIAN)-(OTf)$_2$] (M = Pd, Pt)[29,30] (**1a** and **1b**) ('M') and 1,3-5-tris(pyridyl)-triazine (**tpt**) ('L') in a 6 : 4 M : L ratio (Scheme 1). These are the first Fujita-type M$_6$L$_4$ cages that are soluble in organic media, but not in water. Pd-cage **3a** forms within several hours at r.t. in CH$_2$Cl$_2$, whereas platinum cage **3b** requires longer reaction times, mild heating (40 °C) and MeCN as co-solvent. Cage formation was supported by ^{1}H NMR spectroscopy and X-ray crystallography (for **3a**; see ESI†). DOSY NMR provided a diffusion constant D of 5.37×10^{-10} m^2 s^{-1}, corresponding to a hydrodynamic radius of 1.0 nm,[31] which is in agreement with reported water-soluble M$_6$L$_4$-cages bearing nitrate anions.[32] High resolution cold-spray ionization mass spectrometry (CSI MS) confirmed the elemental composition of **3a** and **3b**, with observable signals for [M(OTf)$_{12}$ − x(OTf)]$^{x+}$ (x = 4–7) (see ESI†).

Cyclic voltammetry (CV) of **3a** provided a reversible reduction and re-oxidation wave around $E_{\frac{1}{2}} = -0.4$ V when scanning to a potential of −1.0 V (*vs.* Fc/Fc$^+$), assigned to the ligand-centered **adi**/**aia**$^{-\bullet}$ redox-couple.[29] Coulometry provided support for reduction of all six BIAN moieties in the first reduction event at −0.4 V in **3a**, with 5.5 electrons transferred per cage (see ESI†). Multiple irreversible redox-events were observed at more cathodic potentials (between −1.2 and −2.2 V *vs.* Fc/Fc$^+$), concomitant with loss in reversibility for the first wave at −0.4 V, suggesting instability of **3a** under more reducing conditions. The model compound **4a**, [Pd(BIAN)(pyr)$_2$](OTf)$_2$ (see ESI† for full characterization) showed almost identical electrochemical responses, indicating (partial) decomposition upon two-electron ligand reduction. Hence, decomposition of cage **3a** appears related to the intrinsically lower stability of Pd(**ada**$^{2-}$) *vs.* Pd(**aia**$^{-\bullet}$) or Pd(**adi**), likely due to more labile Pd–N$_{Py}$ bonds.

We therefore switched to a platinum-based cage, as this should feature stronger metal–ligand bonds.[33] The chemistry of BIAN with Pt is only sparsely developed, particularly when compared to that of Pd.[34] The electrochemistry of the novel bis-pyridine adduct [Pt(BIAN)(pyr)$_2$](OTf)$_2$ **4b** (see ESI† for full characterization, including XRD) indeed shows two reversible reduction events at $E_{1/2} = -0.5$ V and $E_{1/2} = -1.5$ V (Fig. 2). These redox-waves can be assigned to the ligand-based reduction from
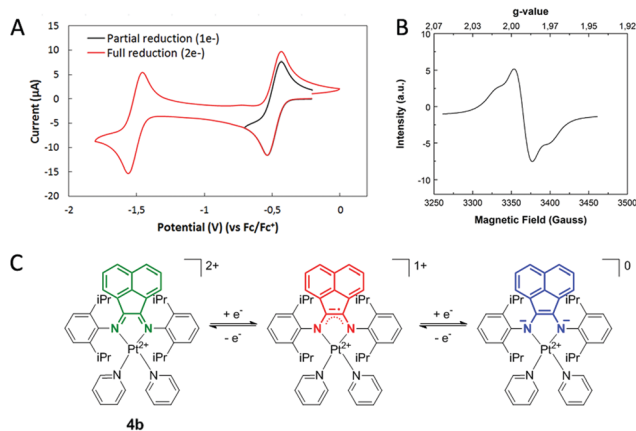

Fig. 2 (A) Cyclic voltammogram of **4b** scanning to −0.7 V (black line) and to −1.8 V (red line) in DCM at 100 mV s^{-1}. (B) EPR spectrum of **4b** after one-electron reduction. (C) Representation of different oxidation states of complex **4b**.

neutral diimino- to imino-amido-radical, *i.e.* [Pt(**adi**)(pyr)$_2$]$^{2+}$ to [Pt(**aia**$^{-\bullet}$)(pyr)$_2$]$^+$, and to the **aia**$^{-\bullet}$/**ada**$^{2-}$ redox-couple, respectively. The complex [Pt(**aia**$^-$)(pyr)$_2$]$^+$ can also be generated using bulk electrolysis or by chemical reduction with CoCp$_2$, making it amenable for *in situ* EPR characterization at r.t. The observed signal is a doublet with $g = 1.99$, which is characteristic for an organic ligand-centered radical (see ESI†).

In line with the excellent stability shown by **4b** across the whole relevant potential window, the new Pt-cage **3b** also showed full electrochemical reversibility between 0 and −2 V. Convolution of the obtained cyclic voltammogram results in the representation depicted in Fig. 3. In agreement with the data obtained for **4b**, the first reduction event (**A**) encountered at −0.5 V is attributed to independent reduction of all six BIAN-ligands present in the nodes of the cage, as no distribution in the redox-potential is observed for this event.

The second redox-event for **3b** (**B**) occurs at $E_{1/2} = -1.3$ V, which is attributed to a **tpt**-centered reduction. In order to get more insight in these reduction events, UV/vis spectro-electrochemistry (SEC-UV/Vis) was performed on cage **3b**, the model complex **4b** and the free organic linker **tpt**. Upon reduction of
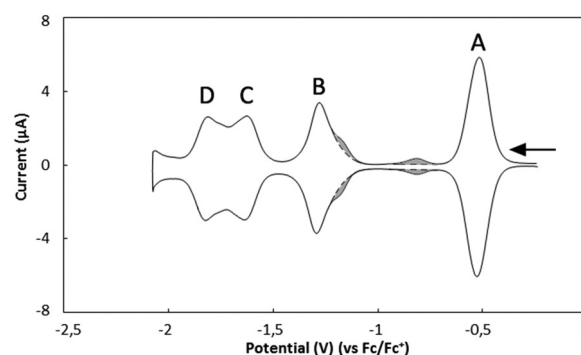

Fig. 3 Semi-derivative convolution plot of BIAN-Pt cage (**3b**) in DCM at 100 mV s^{-1}, demonstrating full reversibility of the supramolecular assembly. Individual reduction processes A–D are labeled above the waves.
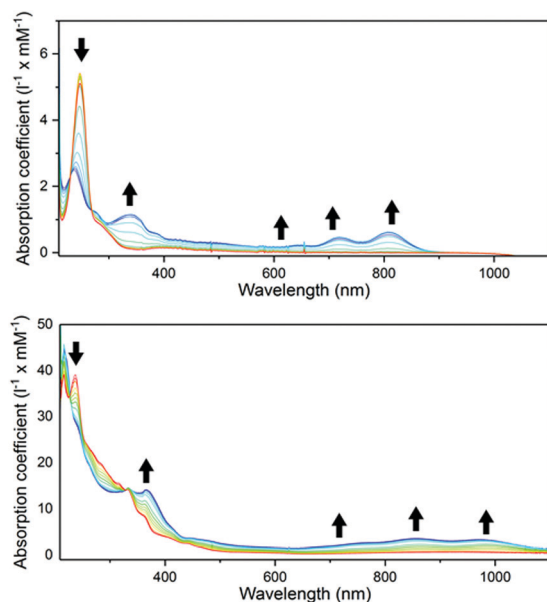
Fig. 4 SEC-UV/Vis of (top) reduction of trispyridyl triazine (**tpt**) to its mono-radical, anionic form (**tpt⁻•**) and (bottom) response of the BIAN-Pt cage (**3b**) during event **B**.
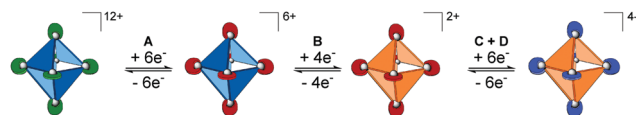

Fig. 5 Schematic representations of the location of the different redox events (**A** to **D**) on the platinum cage.

corresponds to the second BIAN-based redox-event, *i.e.* the $aia^{-•}/ada^{2-}$ couple.

In addition, EPR spectroscopy after bulk electrochemical reduction of **3b** at a potential of −0.7 V (after **A**) provided a signal matching that observed for reduced model complex $[Pt(aia^{-•})(pyr)_2]^+$, confirming that the signal originates from the reduced corner stones (see ESI†). Upon reducing **3b** (fully) to −2.0 V (after **C** + **D**) using bulk electrolysis, this EPR signal virtually disappears. This observation is in line with the hypothesis that the last wave (**C** + **D**) converts the BIAN-cornerstones to their diamagnetic, EPR silent ada^{2-} oxidation state. Lastly, the two subtly different events **C** and **D** (ΔE = 0.18 V), each roughly accounting for the transfer of three electrons, are proposed to arise from changes in the overall charge of the system. In portion **C**, the cage undergoes three BIAN-centred reductions from an overall 2+ to a 1− charge. The reduction of the three remaining BIAN-redox centres in this anionic cage requires a higher cathodic potential, ultimately leading to an overall 4− charge of the cage after event **D**. Thus, cage **3b** exhibits reversible switching from 12+ to 4−, *i.e.* 16 charge-units overall, whilst remaining organic-soluble across the whole redox-regime. These data also show that all of the relevant redox-loci can be independently addressed in the respective reduction processes. The origin of the potential shift between events **C** and **D** might be related to a change from positive/neutral *vs.* negative overall cage charge, to a change in counter-ion (from triflate to tetrabutyl-ammonium) and/or to partial encapsulation of the respective ions.

Cages **3a** and **3b** have an accessible interior volume of 1180 Å³,[37] similar to the water soluble analogues, so guest encapsulation is anticipated if proper interactions with the guest molecule(s) can be established. However, typical guests that bind in water-soluble M_6L_4 cages (*e.g.* adamantane, ferrocene, pyrene or perylene) do not bind in cages **3a** or **3b** in CD_2Cl_2, as deduced from ¹H NMR spectroscopy, likely due to the absence of hydrophobic effects that drive guest encapsulation in water. We therefore switched to $B_{12}F_{12}^{2-}$ as potential guest, as its size and dianionic charge should be complementary to the cage. Upon addition of one equivalent of $B_{12}F_{12}^{2-}$ to either **3a** or **3b**, immediate desymmetrization and broadening of both pyridine signals is observed in the ¹H NMR spectra (see ESI†). The guest is expected to have close contact with the electron poor **tpt**-walls, which causes hindered rotation of the pyridine motifs, leading to desymmetrization and broadening of the signals. The ¹⁹F NMR signal of $B_{12}F_{12}^{2-}$ shifts by 0.4 ppm compared to the free guest in CD_2Cl_2 and using ¹⁹F DOSY NMR a diffusion coefficient of 4.46 × 10⁻¹⁰ m² s⁻¹ was found, in good agreement with the diffusion coefficient of **3b** (see ESI†). We are currently investigating the effects of the redox-switching of the cage on the encapsulation properties of both cages, as reduced electronic interaction or even repulsion between host and the anionic cage may be envisaged upon redox-stimulation of the various organic loci in these assemblies.

3b or **4b**, only minor changes are observed during event **A** (see ESI†). During event **B**, three broad absorptions appear between 600 and 1100 nm, which are very similar to observations made for free **tpt** (Fig. 4).[35,36] This underlines our findings that the **tpt** panels indeed behave as redox-active components that are electronically independent from the BIAN-containing nodes. Hence, event **B** is attributed to the redox-couple **tpt/tpt⁻•** present in the cage construct.

Integration of the redox-waves **A** and **B** leads to a ratio of 1 : 0.67 (Table 1). Given the coulometric data obtained for the first reduction event with **3a**, involving the transfer of six electrons, and because **3b** is present as a single supramolecular assembly with a stoichiometry of M_6L_4, as confirmed by DOSY NMR and HR-MS, the relative CV-integrals thus correspond to a ratio of 6 to 4 for electron-injection in **adi** and **tpt** units, respectively, meaning that each redox-active center present in **3b** independently undergoes well-defined one-electron reduction (**adi/aia⁻•** and **tpt/tpt⁻•**). The first two redox-events in **3b** relate to an overall charge change of the self-assembled cage from 12+ for parent **3b** to 6+ (after event **A**) and subsequently to 2+ (after **B**) (see Fig. 5). Integration of events **C** + **D** relative to **A** results in a near 1 : 1 ratio (0.96 : 1). Given the similar onset redox-potential of −1.63 V compared to the CV of **4b**, this combined wave likely

Table 1 Electrochemical data of **3b** showing the redox-potentials, peak area for each redox-event and their ratios towards the first reduction wave (**A**)

Reduction wave	Peak position (V)	Peak area	Ratio area to **A**	Ratio × 6
A	−0.52 V	6.74 × 10⁻⁷	1.0	6.0
B	−1.28 V	4.63 × 10⁻⁷	0.69	4.1
C + **D**	−1.63 V; −1.81 V	6.44 × 10⁻⁷	0.96	5.8

In summary, we have successfully introduced the known redox-active BIAN-motif into supramolecular 'Fujita-type' coordination cages. This has resulted in the synthesis of two novel, highly charged M_6L_4 cages **3a** and **3b** (M = Pd or Pt) that are soluble in organic solvents and contain redox-active ligands. Decreasing the Pd–N_{Py} bond strength upon two-electron reduction is the likely reason for electrochemical decomposition of Pd-cage **3a**. Pt cage **3b** exhibits full electrochemical stability across the whole potential range of 0 to −2.0 V, with all three oxidation states of the BIAN-ligand reversibly accessible (**adi** ↔ **aia**$^{-\bullet}$ ↔ **ada**$^{2-}$). Furthermore, all four C_3-symmetric trispyridyltriazine wall fragments undergo reversible one-electron reduction (**tpt** ↔ **tpt**$^{-\bullet}$), as deduced from UV/Vis spectro-electrochemistry and coulometry. The cage can be electrochemically reduced in bulk solution, allowing for EPR characterization in different stages of reduction. Cage **3b** can be reversibly switched from overall 12+ to 4− charge, involving storage or release of 16 electrons in total. Initial binding studies with dianionic $B_{12}F_{12}^{2-}$ demonstrate the potential for these organic-soluble cages to form host–guest complexes. We anticipate that these redox stimulus-responsive self-assembled cages may be of interest for application as multi-electron storage devices in *e.g.* non-aqueous redox-flow batteries and for redox-switchable host–guest encapsulation and catalysis.

Conflicts of interest

There are no conflicts to declare.

Notes and references

1 D. L. Caulder, C. Brückner, R. E. Powers, S. König, T. N. Parac, J. A. Leary and K. N. Raymond, *J. Am. Chem. Soc.*, 2001, **123**, 8923.
2 P. Mal, D. Schultz, K. Beyeh, K. Rissanen and J. R. Nitschke, *Angew. Chem., Int. Ed.*, 2008, **47**, 8297.
3 R. Custelcean, P. V. Bonnesen, N. C. Duncan, X. Zhang, L. A. Watson, G. Van Berkel, W. B. Parson and B. P. Hay, *J. Am. Chem. Soc.*, 2012, **134**, 8525.
4 T. K. Ronson, W. Meng and J. R. Nitschke, *J. Am. Chem. Soc.*, 2017, **139**, 9698.
5 J. Mosquera, B. Szyszko, S. K. Y. Ho and J. R. Nitschke, *Nat. Commun.*, 2017, **8**, 14882; W. Cullen, M. C. Misuraca, C. A. Hunter, N. H. Williams and M. D. Ward, *Nat. Chem.*, 2016, **8**, 231.
6 K. Harris, Q. F. Sun, S. Sato and M. Fujita, *J. Am. Chem. Soc.*, 2013, **135**, 12497.
7 M. Tominaga, K. Suzuki, T. Murase and M. Fujita, *J. Am. Chem. Soc.*, 2005, **127**, 11950.
8 R. Gramage-Doria, J. Hessels, S. H. A. M. Leenders, O. Tröppner, M. Dürr, I. Ivanović-Burmazović and J. N. H. Reek, *Angew. Chem., Int. Ed.*, 2014, **53**, 13380.
9 M. Ikemi, T. Kikuchi, S. Matsumura, K. Shiba, S. Sato and M. Fujita, *Chem. Sci.*, 2010, **1**, 68.
10 S. Bivaud, J. Y. Balandier, M. Chas, M. Allain, S. Goeb and M. Sallé, *J. Am. Chem. Soc.*, 2012, **134**, 11968; S. Goeb, S. Bivaud, P. I. Dron, J. Y. Balandier, M. Chas and M. Sallé, *Chem. Commun.*, 2012, **48**, 3106.
11 I. A. Riddell, M. M. J. Smulders, J. K. Clegg, Y. R. Hristova, B. Breiner, J. D. Thoburn and J. R. Nitschke, *Nat. Chem.*, 2012, **4**, 751.
12 P. F. Kuijpers, M. Otte, M. Dürr, I. Ivanović-Burmazović, J. N. H. Reek and B. de Bruin, *ACS Catal.*, 2016, **6**, 3106.
13 Z. J. Wang, C. J. Brown, R. G. Bergman, K. N. Raymond and F. D. Toste, *J. Am. Chem. Soc.*, 2011, **133**, 7358.
14 Q.-Q. Wang, S. Gonell, S. H. A. M. Leenders, M. Dürr, I. Ivanović-Burmazović and J. N. H. Reek, *Nat. Chem.*, 2016, **8**, 225.
15 A. C. H. Jans, A. Gómez-Suárez, S. P. Nolan and J. N. H. Reek, *Chem. – Eur. J.*, 2016, **22**, 14836.
16 D. M. Dalton, S. R. Ellis, E. M. Nichols, R. A. Mathies, F. D. Toste, R. G. Bergman and K. N. Raymond, *J. Am. Chem. Soc.*, 2015, **137**, 10128.
17 R. A. Bilbeisi, J. K. Clegg, N. Elgrishi, X. De Hatten, M. Devillard, B. Breiner, P. Mal and J. R. Nitschke, *J. Am. Chem. Soc.*, 2012, **134**, 5110.
18 T. K. Ronson, W. Meng and J. R. Nitschke, *J. Am. Chem. Soc.*, 2017, **139**, 9698.
19 Y. Ueda, H. Ito, D. Fujita and M. Fujita, *J. Am. Chem. Soc.*, 2017, **139**, 6090.
20 V. Croué, S. Goeb and M. Sallé, *Chem. Commun.*, 2015, **51**, 7275.
21 W. Wang, Y.-X. Wang and H.-B. Yang, *Chem. Soc. Rev.*, 2016, **45**, 2656.
22 A. J. McConnell, C. S. Wood, P. P. Neelakandan and J. R. Nitschke, *Chem. Rev.*, 2015, **115**, 7729.
23 K. Yazaki, S. Noda, Y. Tanaka, Y. Sei, M. Akita and M. Yoshizawa, *Angew. Chem., Int. Ed.*, 2016, **55**, 15031.
24 V. Croué, S. Goeb, G. Szalóki, M. Allain and M. Sallé, *Angew. Chem., Int. Ed.*, 2016, **55**, 1746.
25 G. Szalóki, V. Croué, V. Carré, F. Aubriet, O. Alévêque, E. Levillain, M. Allain, J. Aragó, E. Ortí, S. Goeb and M. Sallé, *Angew. Chem., Int. Ed.*, 2017, **56**, 16272.
26 K. Mahata, P. D. Frischmann and F. Würthner, *J. Am. Chem. Soc.*, 2013, **135**, 15656.
27 M. Yoshizawa, M. Tamura and M. Fujita, *Science*, 2006, **312**, 251; Y. Nishioka, T. Yamaguchi, M. Kawano and M. Fujita, *J. Am. Chem. Soc.*, 2008, **130**, 8160; T. Yamaguchi and M. Fujita, *Angew. Chem., Int. Ed.*, 2008, **47**, 2067; S. H. A. M. Leenders, R. Becker, T. Kumpulainen, B. de Bruin, T. Sawada, T. Kato, M. Fujita and J. N. H. Reek, *Chem. – Eur. J.*, 2016, **22**, 15468.
28 Recent reviews on the use of redox active ligands in catalysis: J. I. van der Vlugt, *Chem. – Eur. J.*, 2019, **25**, 2651; D. L. J. Broere, R. Plessius and J. I. van der Vlugt, *Chem. Soc. Rev.*, 2015, **44**, 6886. See also:D. L. J. Broere, N. P. van Leest, B. de Bruin, M. A. Siegler and J. I. van der Vlugt, *Inorg. Chem.*, 2016, **55**, 8603.
29 R. van Asselt, C. J. Elsevier, C. Amatore and A. Jutand, *Organometallics*, 1997, **16**, 317.
30 W. J. Tao, J. F. Li, A. Q. Peng, X. L. Sun, X. H. Yang and Y. Tang, *Chem. – Eur. J.*, 2013, **19**, 13956.
31 Y. Cohen, L. Avram and L. Frish, *Angew. Chem., Int. Ed.*, 2005, **44**, 520.
32 M. Fujita, D. Oguro, M. Miyazawa, H. Oka, K. Yamaguchi and K. Ogura, *Nature*, 1995, **378**, 469.
33 M. Fujita, F. Ibukuro, K. Yamaguchi and K. Ogura, *J. Am. Chem. Soc.*, 1995, **117**, 4175; D. Fujita, A. Takahashi, S. Sato and M. Fujita, *J. Am. Chem. Soc.*, 2011, **133**, 13317.
34 R. van Asselt, E. Rijnberg and C. J. Elsevier, *Organometallics*, 1994, **13**, 706; C. J. Adams, N. Fey and J. A. Weinstein, *Inorg. Chem.*, 2006, **45**, 6105; M. Shiotsuki, P. S. White, M. Brookhart and J. L. Templeton, *J. Am. Chem. Soc.*, 2007, **129**, 4058; C. J. Adams, N. Fey, M. Parfitt, S. J. A. Pope and J. A. Weinstein, *Dalton Trans.*, 2007, 4446; A. Singh, U. Anandhi, M. A. Cinellu and P. R. Sharp, *Dalton Trans.*, 2008, 2314; T. L. Lohr, W. E. Piers and M. Parvez, *Inorg. Chem.*, 2012, **51**, 4900; T. L. Lohr, W. E. Piers, M. J. Sgro and M. Parvez, *Dalton Trans.*, 2014, **43**, 13858.
35 Contrastingly, for a water-soluble M_6L_4 assembly only one-electron reduction of one **tpt**-unit is reported, proposedly due to strong electronic communication between the redox-loci: Y. Furutani, H. Kandori, M. Kawano, K. Nakabayashi, M. Yoshizawa and M. Fujita, *J. Am. Chem. Soc.*, 2009, **131**, 4764.
36 L. X. Cai, S. C. Li, D. N. Yan, L. P. Zhou, F. Guo and Q. F. Sun, *J. Am. Chem. Soc.*, 2018, **140**, 4869.
37 N. R. Voss and M. Gerstein, *Nucleic Acids Res.*, 2010, **38**, 555.